

# Unsteady Linearized Transonic Flow Analysis for Slender Bodies

D. D. Liu\*

*Northrop Corporation, Hawthorne, Calif.*

M. F. Platzer†

*Naval Postgraduate School, Monterey, Calif.*

and

S. Y. Ruo‡

*Lockheed-Georgia Company, Marietta, Ga.*

An unsteady linearized formulation based on Oswatitsch-Keune's parabolic method is developed to analyze transonic flow past oscillating slender bodies. In contrast to the widely used integral transform method, it is shown that all solutions can be derived by a simpler method directly in the physical plane. By various expansion procedures, low-frequency solutions then are derived according to two clearly defined frequency ranges. Adams-Sears' iteration is employed to account for the second-order effects. Stability derivatives are compared with available theories and data. It is found that the derivatives depend more sensitively on thickness than on the reduced frequency. Finally, a critical assessment of the present method is given.

## Nomenclature

$(x, r, \theta)$	= nondimensional cylindrical coordinates, normalized by the true body length $L$
$U$	= freestream velocity
$t$	= $\tilde{t}L/U$ , nondimensional time
$\tilde{t}$	= true time
$k$	= $\omega L/U$ , reduced frequency
$\omega$	= true angular frequency of pitch
$\Omega, \Phi$	= total and perturbed potentials, both are normalized by $(UL)^{-1}$
$\epsilon$	= maximum body radius/ $L$ , the body thickness ratio

## Introduction

FOR the purposes of guidance, control, and flutter prediction, improved methods of unsteady flow treatment for slender fuselages, and slender bodies/wings often become desirable, particularly during the transonic flight. In the transonic range, large phase lags between the body and the near-field flow possibly may result in low or negative values of damping-in-pitch. The occurrence of such a large phase lag is enhanced mostly by the coupling effect of the steady and unsteady flow, a problem that is far more complicated than those in subsonic and supersonic flights.

In the past, the steady transonic flow problem for an axisymmetric body has been treated by various analytical methods.<sup>1,2</sup> Recent studies of this problem mostly adopted numerical techniques, notably the type sensitive difference scheme,<sup>3</sup> involving the flowfield calculation. However, for the unsteady flow problems, apart from the work appearing in Ref. 4, which is an extension of the earlier work of Liu et al.,<sup>5</sup> little advance has been made for the slender bodies in transonic flow. The purpose of this paper therefore is to develop an efficient, analytical method for deriving the approximate near-field solution for bodies in unsteady transonic flow. The present method, based on the linearized model

according to Oswatitsch-Keune (the parabolic method), accounts globally for the steady thickness effect, in the sense that neither the local steady load nor the transonic shock effect is included. Examination of recent results given by Stahara and Spreiter,<sup>4</sup> however, reveals that, in most cases, little difference exists between the stability derivatives obtained by the local linearization method, and by the parabolic method.<sup>5,6</sup> On the other hand, the present approach consists of the preliminary steps toward a future development of a shock-inclusion method such as Hosokawa's nonlinear correction procedure (e.g., Ref. 5).

Several recent works<sup>19,20</sup> on slender-wing treatments in sonic flow also should be mentioned here, since they also are based on the same extensive concept of parabolic method. Employing the integral method for linearized sonic flow previously developed by Liu<sup>10,16</sup> and Liu et al.,<sup>5</sup> Kimble et al.,<sup>19</sup> and Ruo<sup>20</sup> have derived the slender-wing potential for stability calculation in the low-frequency range. In the present paper, we show that the sonic solution by Ruo can be obtained, directly in the physical space, from combined procedures based on the works of Platzer,<sup>26</sup> Liu,<sup>12</sup> and Zierep.<sup>28</sup> Thus, the cumbersome procedure of the integral transform for deriving not-so-slender-wing/body potentials can be circumvented.

In the following section, we shall present the derivation for the slender-body potentials in the general frequency range. Emphasis will be placed on various approximation procedures and the low-frequency limits of the solution, hence leading to the calculation of the stability derivatives.

## Formulation

Consider a rigid, pointed body of revolution that is exposed to a steady uniform transonic flow. The body performs harmonic, small-amplitude pitching oscillations around its

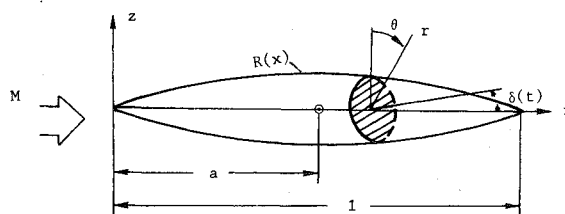


Fig. 1 Body-fixed coordinate system.

Received Aug. 9, 1976; revision received April 4, 1977.

Index categories: Nonsteady Aerodynamics; LV/M Aerodynamics; Transonic Flow.

\*Engineering Specialist, previously with Lockheed-Georgia Company, Advanced Flight Sciences Department. Member AIAA.

†Professor of Aeronautics. Associate Fellow AIAA.

‡R&D Engineer Associate.

nonlifting position (i.e., the steady, mean position). A body-fixed cylindrical coordinate system as shown in Fig. 1 is used to describe the problem.

The equation of state is taken to be that for a perfect gas, and it is assumed that the viscosity and the heat conduction are zero. The body is assumed to be smooth and sufficiently slender so that the small-disturbance concept can be applied. When a body-fixed, cylindrical coordinate system is adopted, a perturbed potential  $\Phi(x, r, \theta, t)$  can be related to the total velocity potential  $\Omega(x, r, \theta, t)$  as follows:

$$\Omega(x, r, \theta, t) = (x-a)\cos\delta + r\sin\delta\cos\theta + \Phi(x, r, \theta, t) \quad (1)$$

where  $\delta = \delta_0 e^{ikt}$ ,  $\delta_0$  is the oscillation amplitude, and  $k$  is the reduced frequency of the pitching motion. The velocity components in the  $x, r$ , and  $\theta$  directions are given by

$$u = \Omega_x = \cos\delta + \Phi_x \quad (2a)$$

$$v = \Omega_r = \sin\delta\cos\theta + \Phi_r \quad (2b)$$

$$w = (1/r)\Omega_\theta = -\sin\delta\sin\theta + (1/r)\Phi_\theta \quad (2c)$$

Then, the time-dependent transonic small-perturbation equation reads

$$\beta^2 \Phi_{xx} + \Phi_{rr} + \frac{1}{r} \Phi_r + \frac{1}{r^2} \Phi_{\theta\theta} - 2M^2 \Phi_{xt} - M^2 \Phi_{tt} = (\gamma + 1) M^2 \Phi_x \Phi_{xx} \quad (3)$$

where  $M$  is the freestream Mach number and  $\beta^2 = 1 - M^2$ . It is a well-known fact that the nonlinear term of Eq. (3) can be ignored only if the flow is sufficiently unsteady or when it becomes purely subsonic or supersonic. We further assume the potential  $\Phi$  to be harmonically time dependent, i.e.,

$$\Phi(x, r, \theta, t) = \phi(x, r) + \varphi(x, r, \theta; \delta_0) e^{ikt} \quad (4)$$

where  $\phi$  is the steady axisymmetric potential and  $\varphi$  is the oscillatory dipole potential. Substituting Eq. (4) into Eq. (3) yields

$$\beta^2 \phi_{xx} + \phi_{rr} + (1/r) \phi_r = (\gamma + 1) M^2 \phi_x \phi_{xx} \quad (5)$$

$$\begin{aligned} \beta^2 \varphi_{xx} + \varphi_{rr} + \frac{1}{r} \varphi_r + \frac{1}{r^2} \varphi_{\theta\theta} - 2ikM^2 \varphi_x \\ + k^2 M^2 \varphi = (\gamma + 1) M^2 (\phi_x \varphi_{xx} + \phi_{xx} \varphi_x) \end{aligned} \quad (6)$$

Notice that the harmonic assumption in Eq. (4) is made possible by the linearization of Eq. (6). Moreover, in arriving at Eqs. (5) and (6), two restrictions are required, i.e.,

$$\tau \ll 1 \text{ and } k\tau \ll 1$$

where  $\tau$  represents either  $\delta_0$  or  $\epsilon$ , the amplitude of oscillation or the body thickness ratio, whichever is larger. (In the present analysis,  $\delta_0$  is always less than  $\epsilon$ , and hence a thickness dominated problem.) Again, the coupling terms on the right-hand side of Eq. (6) cannot be ignored insofar as  $|1 - M^2| = O(\tau^2 \ln \tau)$  and/or  $k = O(\tau^2 \ln \tau)$ . It should be mentioned that, in the case of large-amplitude oscillation, such type of linearization is, of course, not permissible.

Next, to simplify our analysis, the parabolic approximation is used to linearize Eq. (3), i.e.,

$$(\gamma + 1) M^2 \Phi_{xx} = \text{constant} = \Gamma > 0 \quad (7)$$

With this approximation, the model must be restricted to cases in which only slow variations of the steady axial velocity component are admissible. The oscillatory potential  $\varphi$ , on the other hand, can be related to a pulsating source potential  $\hat{\varphi}$  as

$$\varphi(x, r, \theta) = \hat{\varphi}_r(x, r) \cos\theta \quad (8)$$

where  $\hat{\varphi}$  satisfies the following approximate equation, i.e.,

$$\beta^2 \hat{\varphi}_{xx} + \hat{\varphi}_{rr} + (1/r) \hat{\varphi}_r - A \hat{\varphi}_x + k^2 M^2 \hat{\varphi} = 0 \quad (9)$$

where

$$A = \Gamma + 2ikM^2$$

It is seen that the coupling term  $\phi_x \varphi_{xx}$  in Eq. (6) is dropped in Eq. (9). Physically, in the one-dimensional time-dependent model, this amounts to assuming constant slope to the wave characteristics in the  $x, t$  plane. Inclusion of the terms  $\phi_{xx} \varphi_x$  (or  $\Gamma \hat{\varphi}_x$ ) implies that the attenuation mechanism of the wave characteristics is being retained, which thus can provide the low-frequency limit in the present analysis. Also, it should be realized that the inviscid flow assumption is likely to be in error towards the body tail because of the boundary-layer build-up and the possible flow separation.

Hence, in the range of  $0 \leq M \leq 1$ , the pulsating line-source solution of Eq. (9) reads

$$\hat{\varphi}(x, r) = -\frac{1}{4\pi} \int_{-\infty}^{\infty} f(\xi) \cdot \varphi_o(X, r) d\xi \quad (10)$$

and

$$\varphi_o(X, r) = \exp\{\alpha X - [\chi(X^2 + \beta^2 r^2)]^{1/2}\} / (X^2 + \beta^2 r^2)^{1/2} \quad (10a)$$

is an elementary pulsating source solution where

$$\left. \begin{aligned} X &= x - \xi \\ \alpha &= 1/2 A \beta^{-2} \\ \chi &= \alpha^2 - k^2 M^2 \beta^{-2} \end{aligned} \right\} \quad (10b)$$

and  $f(\xi)$  is the line-source distribution function, which can be determined by the tangency condition in the range of interest,  $0 < \xi < 1$ .

For the slender-body approximation of Eq. (10), the pulsating solution can be written in two terms, i.e.,<sup>§</sup>

$$2\pi \hat{\varphi}(x, r) = f(x) \ln r + \hat{\varphi}_R(x; k) + O(r^2 \ln r) \quad (11)$$

By means of the method of elementary steps proposed by Keune (e.g., Ref. 7) and Platzer & Hoffman,<sup>8</sup>  $\hat{\varphi}_R$  can be obtained as

$$\begin{aligned} \hat{\varphi}_R(x; k) = & -\frac{1}{2} \left( \frac{\partial}{\partial x} + \sqrt{\chi} - \alpha \right) \int_0^x f(\xi) e^{-(\sqrt{\chi} - \alpha)\xi} \ln \chi d\xi \\ & + \frac{1}{2} \left( \frac{\partial}{\partial x} - \sqrt{\chi} - \alpha \right) \int_x^1 f(\xi) e^{-(\sqrt{\chi} + \alpha)|X|} \ln |X| d\xi + f(x) \ln \frac{\beta}{2} \end{aligned} \quad (11a)$$

Equation (11) implies an extension of the equivalence rule by Oswatitsch and Keune<sup>9</sup> to pulsating flow, see also Platzer.<sup>26</sup> The first term is the "crossflow" term which only accounts for the incompressible effect due to the area variation. The second term  $\varphi_R$  is the "spatial influence" term which depicts the compressibility effect describing the influence of body pulsation upstream and downstream of the crossflow plane. When  $k$  is set to zero in Eq. (11a),  $\sqrt{\chi} = \alpha = \Gamma/2\beta^2$ ,  $\varphi_R$  thus reduces to the steady solution ob-

<sup>§</sup>In the nonlinear analysis, the lower order term of  $O(r^2 \ln r)$  is a term of  $O(r^2 \ln^2 r)$ . However, since our analysis is based on the linearized equation,  $O(r^2 \ln r)$  terms naturally do not appear. Also,  $O(r^2 \ln r)$  should be written formally as  $O(k^2 r^2 \ln kr)$  for the frequency ratio  $0 < k < 1$  and as  $O(k^4 r^2 \ln k^2 r)$ , for  $k > 1$ .

tained by Maeder and Thommen<sup>22</sup> via integral transform, i.e.,

$$\varphi_R(x;0) = -\frac{1}{2} \frac{\partial}{\partial x} \int_0^x f(\xi) \ln X d\xi + \frac{1}{2} \left( \frac{\partial}{\partial x} - 2\alpha \right) \int_x^l f(\xi) e^{2\alpha X} \ln |X| d\xi + f(x) \ln(\beta/2) \quad (12)$$

### Oscillatory Flow

For the derivation of the oscillatory slender-body potential, we mention two different approaches. The first approach is the commonly used method of integral transform. Fourier transformation of Eq. (9) in the  $x$  direction gives

$$\bar{\varphi}_{rr} + (1/r) \bar{\varphi}_r - \lambda^2 \bar{\varphi} = 0 \quad (13)$$

where

$$\bar{\varphi}(u,r) = \frac{1}{\sqrt{2\pi}} \int_{-\infty}^{\infty} e^{-iux} \hat{\varphi}(x,r) dx$$

and

$$\lambda^2 = \beta^2 u^2 + (2kM^2 - i\Gamma)u - k^2 M^2$$

Applying Sommerfeld's radiation condition yields the solution in the transformed plane,

$$\bar{\varphi}(u,r) = -\bar{f}(u) K_0(\lambda r) \quad (14a)$$

Expanding the modified Bessel function  $K_0(\lambda r)$  for small argument of  $\lambda r$ , and retaining terms up to order  $O(\lambda^2 r^2 \ln \lambda r)$  and  $O(\lambda^2 r^2)$ , and after Fourier inversion of these terms, lastly applying the relation Eq. (8), then gives the oscillatory dipole solution, i.e.,

$$\varphi(x,r,\theta) = \frac{\partial}{\partial r} \left[ \frac{1}{\sqrt{2\pi}} \int_{-\infty}^{\infty} e^{ixu} \bar{\varphi}(u,r) du \right] \cdot \cos\theta = \frac{F(x)}{2\pi r} \cos\theta + \zeta[x,r,\theta;\Gamma,k] + O(k^4 r^3 \ln kr) \quad (14b)$$

and

$$\begin{aligned} \zeta[x,r,\theta;\Gamma,k] = & \frac{\text{Arcos}\theta}{8\pi} \left\{ F'(x) \left[ \ln \frac{r^2}{2} + N(\Gamma,k) \right] \right. \\ & - \frac{\partial^2}{\partial x^2} \int_0^x F(\xi) \ln X d\xi \left. - \frac{k^2 r \cos\theta}{8\pi} \left\{ F(x) \left[ \ln \frac{r^2}{2} + N(\Gamma,k) \right] \right. \right. \\ & \left. \left. - 2 \frac{\partial}{\partial x} \int_0^x F'(\xi) \ln X d\xi + \frac{\partial^2}{\partial x^2} \int_0^x F(\xi) X \ln X d\xi \right\} \right\} \quad (14c) \end{aligned}$$

where

$$N(\Gamma,k) = \frac{1}{2} \ln \left( k^2 + \frac{\Gamma^2}{4} \right) + C - 1 + i \left[ \frac{\pi}{2} - \tan^{-1} \left( \frac{\Gamma}{k} \right) \right]$$

and  $C = 0.5772 \dots$ , Euler's constant.

The details of the inverse Fourier transform can be found in Ref. 10. It is noted that further expansion of  $N(\Gamma,k)$  according to the low-frequency expansion criterion (see next section) yields identically the low-frequency solutions Eqs. (17) and (19).

The second approach is a much simpler, yet unified one, by which the same solution can be generated in the physical plane within a few steps. We first recast Eq. (9) in the following form,

$$\hat{\varphi}_{rr} + (1/r) \hat{\varphi}_r = \Lambda \hat{\varphi} \quad (15)$$

where  $\Lambda$  is the operator defined as

$$\Lambda = -\beta^2 \frac{\partial^2}{\partial x^2} - A \frac{\partial}{\partial x} + k^2 M^2 \quad (15a)$$

Now, substituting  $\varphi$  from Eq. (11) into the right-hand side of Eq. (15), then performing integration of Eq. (15) in  $r$ , and finally making use of relation (8), immediately yields the slender-body oscillatory dipole solution, i.e.,

$$\begin{aligned} \varphi(x,r,\theta) = & \frac{F(x)}{2\pi r} \cos\theta + \frac{r \cos\theta}{8\pi} \Lambda \\ & \cdot \left\{ - \left( \frac{\partial}{\partial x} + \sqrt{\chi} - \alpha \right) \int_0^x F(\xi) e^{-(\sqrt{\chi}-\alpha)X} \ln X d\xi \right. \\ & + \left( \frac{\partial}{\partial x} - \sqrt{\chi} - \alpha \right) \int_x^l F(\xi) e^{-(\sqrt{\chi}+\alpha)|X|} \ln |X| d\xi \\ & \left. + F(x) \left( \ln \frac{\beta^2 r^2}{4} - 1 \right) \right\} \quad (16) \end{aligned}$$

where  $F(\xi)$  denotes the dipole distribution function, to be determined from the Adams-Sears iterative procedure from the tangency condition.

It is seen that the combined procedure of Platzer-Hoffman's "elementary step"<sup>8</sup> [Eq. (8a)] and the "simple approach" by Liu<sup>12</sup> [Eq. (13)] constitutes a greatly simplified procedure as opposed to the commonly used integral transform method. This combined procedure requires no knowledge of the inversion transform, as it can be operated directly in the physical plane. Furthermore, it is a unified method for subsonic, transonic, and supersonic potential flow, insofar as the equation is linear. However, we shall not elaborate on the derivation of this approach here. The detail and the verification of this approach will be published elsewhere.<sup>12</sup>

For the case of  $\Gamma = 0$ ,  $\sqrt{\chi} = \alpha/M$ , Eq. (13) reduces to the purely subsonic dipole solution [Eq. (8), Ref. 13]. It also contains the sonic flow solution as a special case, since  $\sqrt{\chi} + \alpha$  approaches infinity and  $\sqrt{\chi} - \alpha = -k^2/A$  as  $M$  approaches unity.

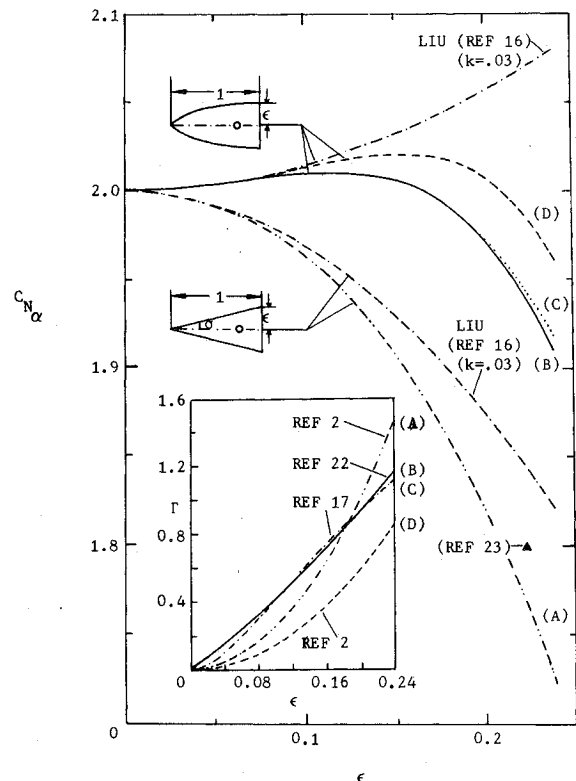


Fig. 2 Effect of thickness ratio on the normal force coefficient slope for a cone and for a parabolic ogive (subdiagram: determination of  $\Gamma$ ) at  $M = 1.0$ .

### Low-Frequency Sonic Solution

To demonstrate the present expansion method, we perform the analysis only in the sonic flow range (i.e.,  $M$  is equal to or near one). We further confine the reduced frequency  $k$  to be a parameter which is smaller than unity. Next, we define two parameters,  $\nu$  and  $\mu$ , where  $\nu = \Gamma/k$  and  $\mu = k/\Gamma$ . According to the range of these parameters, two cases are of interest, namely the moderately low frequency range and the very low frequency range. The expanded solutions are discussed as follows.

#### Moderately-Low Frequency Cases: $\nu O(1)$

In this case, the body is assumed to be "sufficiently" thin and the reduced frequency, "not too low" such that  $\nu = O(1)$ ; hence, this is equivalent to stating that  $k = O(\epsilon^2 \ln \epsilon)$ . Also, the quadratic and the product terms of the parameters  $\nu$ ,  $\Gamma$ , and  $k^2$  are negligibly small, then Eq. (13) can be expressed to yield the following solution

$$\begin{aligned} \varphi(x, r, \theta) = & \frac{F(x)}{2\pi r} \cos\theta - \frac{\Gamma r \cos\theta}{8\pi} \left\{ F'(x) \left[ \ln \frac{kr^2}{2} + C + \frac{i\pi}{2} \right] \right. \\ & - \frac{\partial^2}{\partial x^2} \int_0^x F(\xi) \ln X \, d\xi \left. \right\} + \frac{ikr \cos\theta}{4\pi} \\ & \cdot \left\{ F'(x) \left[ \ln \frac{kr^2}{2} + C - I - \frac{i\pi}{2} \right] - \frac{\partial^2}{\partial x^2} \int_0^x F(\xi) \ln X \, d\xi \right\} \\ & - \frac{k^2 r \cos\theta}{4\pi} \left\{ F(x) \left[ \ln \frac{kr^2}{2} + C - I + \frac{i\pi}{2} \right] \right. \\ & - 2 \frac{\partial}{\partial x} \int_0^x F(\xi) \ln X \, d\xi + \frac{\partial^2}{\partial x^2} \int_0^x F(\xi) X \ln X \, d\xi \left. \right\} \\ & + O(k^4 r^3 \ln kr) \end{aligned} \quad (17)$$

For vanishingly small  $\nu$ , i.e.,  $\Gamma = o(k)$ , the preceding solution reduces to the sonic solution previously obtained by Hsu and Ashley.<sup>14</sup> By further restricting the reduced frequency to be only high enough so that the second-order terms in  $k$  can be ignored, we then recover Landahl's<sup>15</sup> linearized solution, i.e.,

$$\begin{aligned} \varphi(x, r, \theta) = & \frac{F(x)}{2\pi r} \cos\theta + \frac{ikr \cos\theta}{4\pi} \left\{ F'(x) \ln \frac{kr^2}{2} + C - I \right. \\ & + \frac{i\pi}{2} - \frac{\partial^2}{\partial x^2} \int_0^x F(\xi) \ln X \, d\xi \left. \right\} + O(k^2 r \ln kr) \end{aligned} \quad (18)$$

This solution also was employed by Liu<sup>16</sup> for the stability derivative calculation shown in Figs. 2, 4, and 5. Notice that Eqs. (17) and (18) both contain a logarithmic term in  $k$ . Thus, it is expected that the stability derivatives based on these solutions do not contain a low-frequency limit (see Fig. 5).

#### Very-Low Frequency Case: $\mu = o(1)$

Assume now that the body is oscillating at a very low frequency such that  $\mu = o(1)$ , i.e.,  $k = o(\epsilon^2 \ln \epsilon)$ , and that the quadratic and the product terms of the parameters  $\mu$  and  $k$  are negligibly small. Then Eq. (14) can be expanded to yield

$$\begin{aligned} \varphi(x, r, \theta) = & \frac{F(x)}{2\pi r} \cos\theta + \frac{\Gamma r \cos\theta}{8\pi} \left\{ F'(x) \left[ \ln \frac{\Gamma r^2}{4} + C - I \right] \right. \\ & - \frac{\partial^2}{\partial x^2} \int_0^x F(\xi) \ln X \, d\xi \left. \right\} + \frac{ikr \cos\theta}{4\pi} \left\{ F'(x) \left[ \ln \frac{\Gamma r^2}{4} + C \right] \right. \\ & - \frac{\partial^2}{\partial x^2} \int_0^x F(\xi) \ln X \, d\xi \left. \right\} + O(k^2 r \ln kr) \end{aligned} \quad (19)$$

Note that this solution is linearly dependent on  $k$  and is a counterpart of the supersonic low-frequency solution.<sup>6</sup> It is this solution which we shall employ mainly for the calculation of stability derivatives in the next section.

Other than by the expansion method described earlier, the same very low frequency solution (16) can be derived by alternative methods directly from the low frequency form of Eq. (9). The explicit sonic solution satisfying the low frequency form of Eq. (9) reads

$$\hat{\varphi}(x, r) = - \frac{1}{4\pi} \int_0^x F(\xi) \cdot \varphi_o(X, r) \, d\xi \quad (20)$$

and

$$\varphi_o(X, r) = \exp[-Ar^2/X]/X \quad (20a)$$

These methods are based on the expansion of either the distribution function  $F(\xi)$  or the kernel function  $\varphi_o(X, r)$ . The latter method requires the use of Mangler's improper integral which finally leads to Eq. (15). A more meaningful result is provided by the former method, in that an infinite-series form of Eq. (15) can be obtained. Since the series form is pertinent to our later stability derivative calculation, the essential steps are sketched as follows.

According to Hosokawa,<sup>17</sup> a transformed variable  $u$  can be introduced, i.e.,

$$u = Ar^2/4K \quad (21)$$

for the sonic slender-body approximation.

When Eq. (20) is transformed by Eq. (21) and  $F(\xi)$  is expanded in Taylor series around  $\xi = x$ , one obtains

$$\hat{\varphi}(x, r) = - \frac{1}{4\pi} \sum_{n=0}^{\infty} \frac{(-1)^n}{n!} F^{(n)}(x) \left( \frac{Ar^2}{4} \right) \cdot J_{n+1} \left( \frac{r^2}{x} \right) \quad (22)$$

where

$$J_n(r^2/x) = \int_{(Ar^2/4x)}^{\infty} \frac{e^{-u}}{u^n} \, du \quad (22a)$$

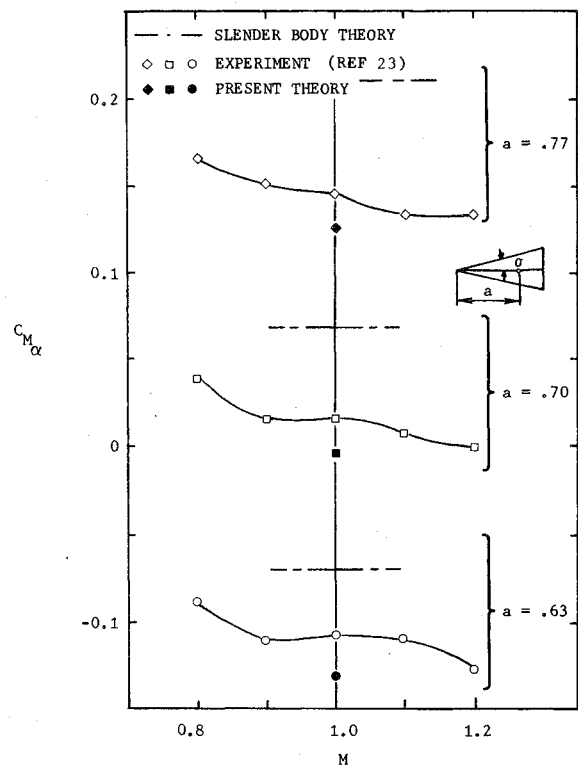


Fig. 3 Pitching moment slope for a cone ( $\sigma = 12.5^\circ$ ) at  $M = 1.0$ .

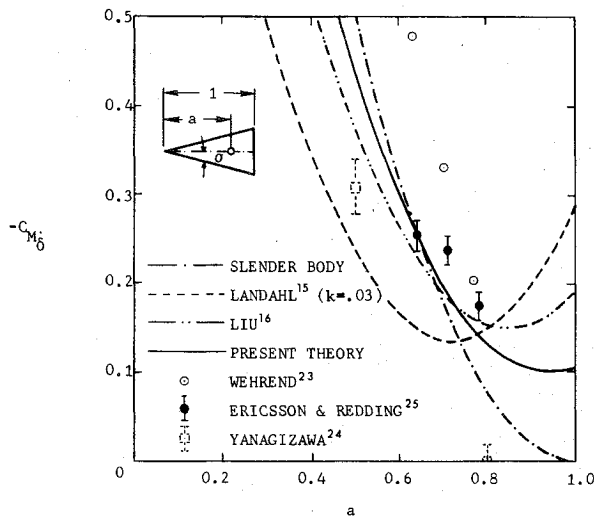


Fig. 4a Effect of pitch-axis location on the damping moment for a cone ( $\sigma = 12.5^\circ$ ) at  $M = 1.0$ .

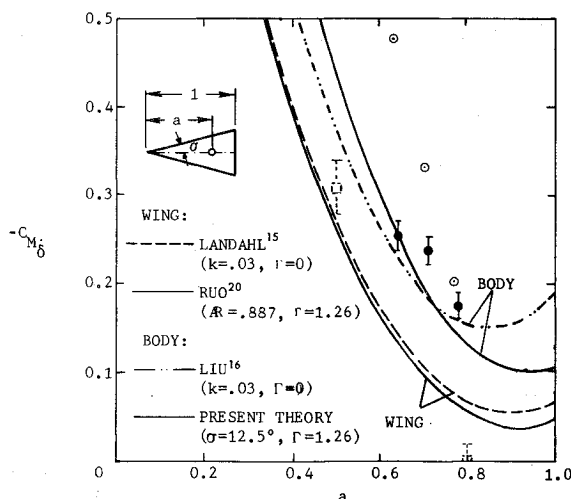


Fig. 4b Comparison of the damping moments for a cone ( $\sigma = 12.5^\circ$ ) and for an "equivalent" delta wing ( $R = 1.13$ ) at  $M = 1.0$ .

Making use of the recurrence formula of  $J_n(r^2/x)$  in Ref. 17 and of relation (8) yields the very low frequency series solution after some manipulation:

$$\begin{aligned} \varphi(x, r, \theta) = & \frac{F(x)}{2\pi r} \cos\theta + \frac{\Gamma r \cos\theta}{8\pi} \left[ F'(x) \left( \ln \frac{\Gamma r^2}{4x} + C \right) \right. \\ & - \frac{F(x)}{x} - \sum_{n=2}^{\infty} \frac{F^{(n)}(x)}{n!(n-1)} (-x)^{n-1} \left. \right] \\ & + \frac{ikr \cos\theta}{4\pi} \left[ F'(x) \left( \ln \frac{\Gamma r^2}{4x} + C + I \right) \right. \\ & - \frac{F(x)}{x} - \sum_{n=2}^{\infty} \frac{F^{(n)}(x)}{n!(n-1)} (-x)^{n-1} \left. \right] \end{aligned} \quad (23)$$

From a programming standpoint, Eq. (23) is a more convenient form than Eq. (19), particularly for the power-law bodies. For details of this distribution-function expansion method, refer to Ref. 11.

### Slender-Wing Extension

The present slender-body analysis has an important extension to the case of slender-wing (or wing-body com-

bination) solution in accordance with the equivalence rule. For example, as related to the given downwash  $w(x, y, 0; k)$  at the wing planform, solution (14b) can be recast simply in the following form, i.e.,

$$\begin{aligned} w(x, y, 0; k) = \varphi_z(x, y, 0) = & -\frac{1}{\pi} \int_{-S(x)}^{S(x)} \frac{\varphi_\eta(x, \eta, 0)}{y - \eta} d\eta \\ & + \zeta[\varphi; \Gamma, k] + O([k\sigma^2 \ln k\sigma^2]^2) \end{aligned} \quad (24)$$

where  $S(x)$  is the half-span,  $\sigma$  is the semispan-to-chord ratio, and  $\eta$  is the spanwise dipole location.

The first term of Eq. (24) is the Munk-Jones term, corresponding to the first term of Eq. (14b), whereas the second term of Eq. (24) can be obtained conveniently from the second term of Eq. (14b) in replacing  $r \cos\theta$  by  $z$ ,  $r$  by

$$\sqrt{(y - \eta)^2 + z^2}, \text{ and } F(x) \text{ by } \int_{-S(x)}^{S(x)} \varphi(x, \eta, 0) d\eta$$

then differentiating it with respect to  $z$ , and letting  $z$  approach zero, i.e.,

$$\begin{aligned} \zeta[\varphi; \Gamma, k] = & \frac{A}{4\pi} \frac{\partial}{\partial x} \left\{ \left[ \ln \frac{1}{2} + N(\Gamma, k) \right] \cdot \Pi[x, S(x)] \right. \\ & + 2 \int_{-S(x)}^{S(x)} \varphi \ln |y - \eta| d\eta \left. \right\} - \frac{A}{4\pi} \frac{\partial^2}{\partial x^2} \left\{ \int_0^x \ln X \cdot \Pi[\xi, S(\xi)] d\xi \right. \\ & - \frac{k^2}{4\pi} \left\{ \left[ \ln \frac{1}{2} + N(\Gamma, k) \right] \cdot \Pi[x, S(x)] - 2 \frac{\partial}{\partial x} \int_0^x \ln X \right. \\ & \left. \left. \cdot \Pi[\xi, S(\xi)] d\xi + \frac{\partial^2}{\partial x^2} \int_0^x X \ln X \cdot \Pi[\xi, S(\xi)] d\xi \right\} \right. \end{aligned} \quad (24a)$$

where

$$\Pi[\xi, S(\xi)] = \int_{-S(\xi)}^{S(\xi)} \varphi(\xi, \eta) d\eta$$

When  $\Gamma$  is set to zero, Eq. (24) reduces to Landahl's solution<sup>18</sup> as a special case. Eq. (24) has been derived separately by Kimble et al.,<sup>19</sup> and by Ruo<sup>20</sup> using the integral transform technique. When a proper expansion is performed

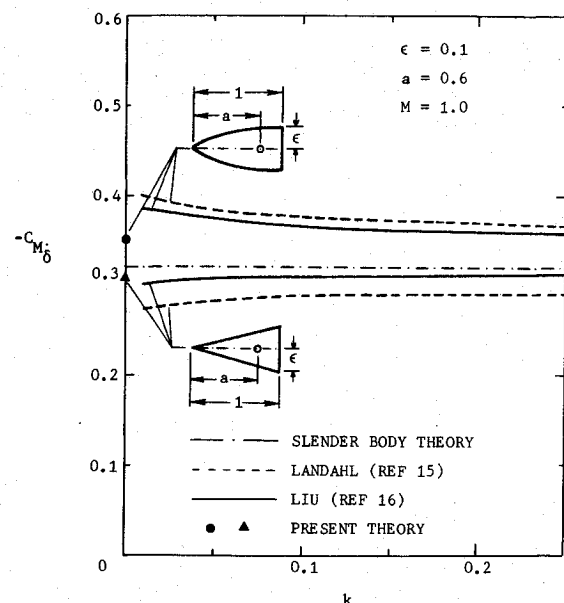


Fig. 5 Effect of reduced frequency on the damping moments for a cone and for a parabolic ogive at  $M = 1.0$ .

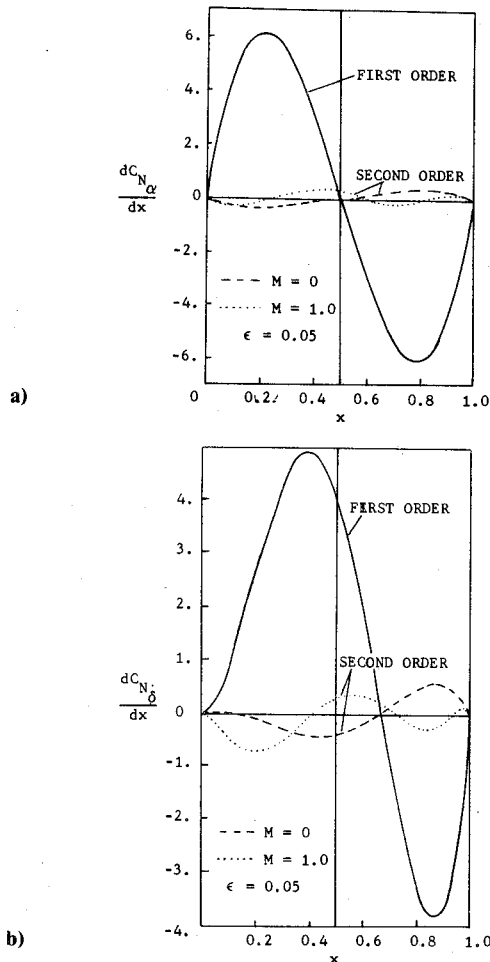


Fig. 6 Normal forces for a parabolic spindle at  $M=0$  and  $M=1.0$ . a) In phase; b) Out-of-phase.

according to the very low frequency approximation,  $N$  becomes  $N(\Gamma, k) \approx \ln(\Gamma/2) + C - 1 + 2i\mu$ . The very low frequency slender-wing solution can be obtained by dropping the higher-order terms in  $k$  in the expanded form of Eq. (24a). Ruo<sup>20</sup> has employed the solution for the stability analysis of a delta wing. Some results will be compared in the next section with the slender-body results (Fig. 4b).

Furthermore, we note that these solutions are strictly near-field solutions, in the sense that the lifting effect is much smaller than the thickness effect (i.e.,  $\delta_o \ll \epsilon$ ). Hence, it justifies our omission of the nonlinear contribution in the outer flow resulting from different degrees of lift control.<sup>21</sup>

### Stability Derivatives

Adams-Sears' iterative procedure<sup>29</sup> is introduced first to determine the dipole distribution  $F(\xi)$  along  $r=R(x)$ . The specific details of this procedure can be found in our earlier reports.<sup>6,8,13</sup> Here we merely describe the essential steps.

According to the different order of thickness, the downwash  $W(x)$ , the dipole function  $F(x)$ , and dipole potential  $\chi(x, r)$ , defined as  $\chi = \phi_r$ , are split in the following manner:

$$\Pi \approx \Pi^{(1)+(2)} \equiv \Pi^{(1)} + \Pi^{(2)} \quad (25)$$

where  $\Pi$  symbolically represents  $W(x)$ , or  $F(x)$ , or  $\chi(x, r)$ , the first-order term  $\Pi^{(1)}$  represents the Munk-Jones approximation (the so-called slender-body theory), and the second-order term  $\Pi^{(2)}$  is the thickness correction term related to the first-order term by the tangency condition

$$\chi_r = -W(x) + R'(x)\chi_x \quad \text{at } r=R(x) \quad (26a)$$

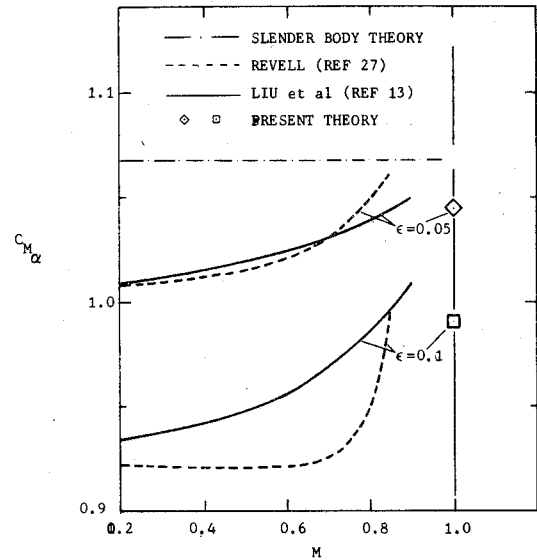


Fig. 7 Effect of Mach number and thickness ratio on the stiffness moment for a parabolic spindle.

and  $W(x)$  now describes the rigid body motion

$$W = \{\xi + \delta\bar{x}\} + \left\{ \frac{Q'(x)}{2\pi} \delta \right\} \quad (26b)$$

where  $\bar{x} = x - a$ , and  $a$  is the pitching-axis location,  $Q(x)$  is the body cross-section area, and  $\delta = ik\delta$ . After much manipulation, one obtains the dipole potential

$$\chi^{(1)+(2)} = \delta\psi^{(1)+(2)} + \delta\lambda^{(1)+(2)} \quad (27)$$

where the in-phase potential and the out-of-phase potential read, respectively,

$$\begin{aligned} \psi^{(1)+(2)} = & \frac{Q(x)}{\pi r} [I + Z_R] - \frac{Q'^2(x)}{2\pi^2 r} \\ & - r \left[ V_R \ln \frac{\Gamma r^2}{4} + Y_R \right] + O(\epsilon^5 \ln \epsilon) \end{aligned} \quad (27a)$$

$$\begin{aligned} \lambda^{(1)+(2)} = & \frac{Q(x)}{\pi r} [\bar{x} + Z_I] - \frac{Q'^2(x)}{2\pi^2 r} \bar{x} \\ & - r \left[ V_I \ln \frac{\Gamma r^2}{4} + Y_I \right] + O(\epsilon^5 \ln \epsilon) \end{aligned} \quad (27b)$$

and

$$V_R = \frac{\Gamma}{4\pi} Q'(x), \quad V_I = \frac{\Gamma}{4\pi} [\bar{x} Q'(x) + Q(x)] + \frac{Q'(x)}{2\pi} \quad (27c)$$

$$Y_R = \frac{\Gamma}{4\pi} [(C-1)Q'(x) - \int_0^x Q''(\xi) \ln X d\xi] \quad (27d)$$

$$\begin{aligned} Y_I = & \frac{\Gamma}{4\pi} \{ (C-1)[\bar{x} Q'(x) + Q(x)] - \int_0^x [\xi Q''(\xi) \\ & + 2Q'(\xi)] \ln X d\xi \} + \frac{1}{2\pi} \{ CQ'(x) - \int_0^x Q''(\xi) \ln X d\xi \} \end{aligned} \quad (27e)$$

$$Z_R = V_R \left[ 2 + \ln \frac{\Gamma r^2}{4} \right] + Y_R, \quad Z_I = V_I \left[ 2 + \ln \frac{\Gamma r^2}{4} \right] + Y_I \quad (27f)$$

The linearized Bernoulli's equation gives the expressions for the in-phase and out-of-phase pressure coefficients in

association with  $\delta$  and  $\delta$ , up to  $O(\epsilon^5 \ln \epsilon)$ , respectively:

$$C_{p1} = -2\psi^{(1)+(2)} - R'^2(x) \cdot \psi_x^{(1)} \quad (28a)$$

$$C_{p2} = -2(\lambda_x + \psi)^{(1)+(2)} + 2[\psi^{(1)} + R(x)]\phi_x^{(1)} - R'^2(x)[\lambda_x^{(1)} - \psi^{(1)} - 2R(x)] \quad (28b)$$

where  $\phi_x^{(1)}$  is the steady flow velocity, based on the slender-body approximation,<sup>1</sup>

$$\phi_x^{(1)}(x, r) = \frac{1}{4\pi} \left\{ Q'(x) \left( \ln \frac{\Gamma r^2}{4} + C \right) - \int_0^x Q''(\xi) \ln X d\xi \right\} \quad (28c)$$

or based on its local linearization solution<sup>2</sup> for the case of a cone. Thus, the stability derivatives, up to  $O(\epsilon^4 \ln \epsilon)$ , can be evaluated from the following formulas, i.e.,

Stiffness derivatives

$$C_{N\delta} = -I_1[C_{p1}] \text{ and } C_{M\delta} = I_2[C_{p1}] \quad (29a)$$

Damping derivatives

$$C_{N\dot{\delta}} = -I_1[C_{p2}] \text{ and } C_{M\dot{\delta}} = I_2[C_{p2}] \quad (29b)$$

where  $I_1$  and  $I_2$  are the integral operator defined as

$$I_1[ ] = \frac{\pi}{Q(I)} \int_0^I R[ ] dx$$

and

$$I_2[ ] = \frac{\pi}{Q(I)} \int_0^I (\bar{x}R + R^2 R') [ ] dx \quad (29c)$$

Much detail concerning the derivation and the evaluation of Eqs. (27-29) can be found in the report by Ruo and Liu.<sup>6</sup>

### Determination of $\Gamma$

For numerical computations, the value of the acceleration constant  $\Gamma$  must be determined. Throughout the calculation several different  $\Gamma$  values based on the local linearization method<sup>2</sup> (curves A and D, Fig. 2), Hosokawa's method<sup>17</sup> (curve B), and the method of Maeder and Thommen<sup>22</sup> (curve C) were adopted. Hosokawa's method appears to be particularly appropriate, as  $\Gamma$  can be "uniquely" determined by the following conditions, i.e.,

$$\phi_x(x^*; \Gamma) = \frac{1 - M^2}{(\gamma + 1)M^2} \text{ and } \phi_{xx}(x^*; \Gamma) = \frac{\Gamma}{(\gamma + 1)M^2} \quad (30)$$

Thus,  $x^*$ , the sonic point, and  $\Gamma$  can be obtained in solving these algebraic equations together with the steady solution given in Eq. (28c). Again, for further details one should refer to Ref. 6.

For the calculation of an "equivalent" wing, Zierep<sup>28</sup> has shown that the equivalence rule, in the sense of the parabolic method, assures that the same  $\Gamma$  value can be used for wings and bodies having the same cross-sectional area at the respective axial locations. Its application to unsteady flow calculations was pointed out earlier by the first author (D.D. Liu) and subsequently was adopted to the wing calculations by Kimble et al.<sup>19</sup> and Ruo<sup>20</sup> (see Fig. 4b).

### Results and Discussions

To illustrate the effects of Mach number, thickness ratio, body geometry, and pitch axis location on the static and dynamic stability derivatives, numerical examples were calculated for three different configurations, namely, 1) right circular cone:  $R(x) = \epsilon x$ ; 2) parabolic ogive:  $R(x) = \epsilon(2 - x)$ ; and 3) parabolic spindle:  $R(x) = 4\epsilon x(1 - x)$  for  $0 \leq x \leq 1$ . Most of the results shown here, unless otherwise stated, are based on Eq. (19) or Eq. (23), evaluated at or near the Mach

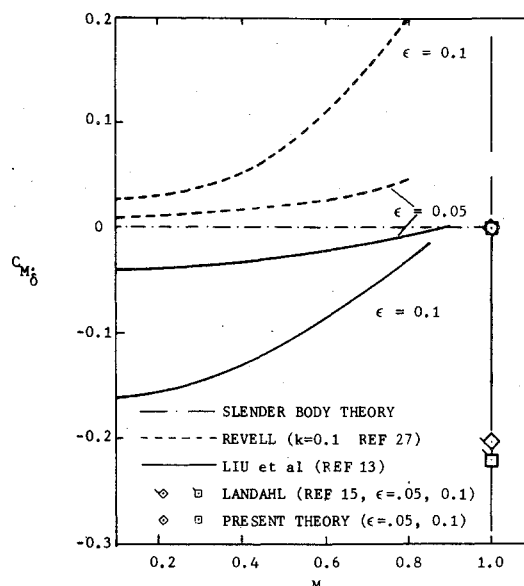


Fig. 8 Effect of Mach number and thickness ratio on the damping moment for a parabolic spindle at  $\alpha = 0$ .

number equal to unity. Figure 2 shows the effect of thickness on the normal force coefficient slope based on different  $\Gamma$  values. In Fig. 3, the pitching moment coefficient slope of a 12.5-deg cone is compared with Wehrend's<sup>23</sup> test result showing considerable improvements over the slender body theory predictions. In Fig. 4a we compare the damping-in-pitch moment vs pitch-axis location for a 12.5 deg cone with experimental data provided by Wehrend<sup>23</sup> and Yanagizawa.<sup>24</sup> Ericsson and Redding's correction<sup>25</sup> further brings Wehrend's data closer to the present result. In Fig. 4b the damping-in-pitch for a cone and for a delta wing, based on various theories are presented. The comparison is made between slender wings and bodies for configurations of the same virtual mass; hence, this amounts to the local span variation of the wing  $S(x)$  being equal to the local radius  $R(x)$  of the body under consideration. In this case the aspect ratio of the delta wing thus is related to the cone thickness as  $R = 4\epsilon$ . It is seen in Fig. 4b that the cone gains more negative damping than the delta wing does at sonic speed. Figure 5 exhibits the damping-in-pitch for a cone and a parabolic ogive in the low-frequency range. It is interesting to note that the recent result calculated by Stahara and Spreiter<sup>4</sup> appears to be almost indistinguishable from our very low-frequency results. Their result also approaches Liu's result<sup>16</sup> in the moderately low-frequency range as  $k$  increases.

In Figs. 6-8 some results for a parabolic spindle are presented. Ordinarily, in steady sonic flow such a configuration will produce a standing shock wave on the body. Although we are aware of this fact, the present formulation does not include the unsteady shock calculation. To provide a preliminary result, we feel that it is practical at this time to make use of the "smooth" sonic solution<sup>22</sup> for estimates of the global values such as damping forces and moments. Thus, Fig. 6 indicates the different order effect for the in- and out-of-phase local force variation for a spindle at  $M=0$  and  $M=1$ . Similar to the nonlifting pressure distribution, the in-phase  $dC_{N\alpha}/dx$  is symmetrical (WRT  $x=1/2$ ) for all the subsonic cases but asymmetrical for the transonic cases. Figures 7 and 8 show the stiffness derivative and the damping derivative at  $M=1$  in conjunction with our previous subsonic results.<sup>5,13</sup> In passing, it should be mentioned that in the subsonic regime, Revell's result<sup>27</sup> was based on inhomogeneous equations which consistently account for the thickness effects due to the steady mean flow, whereas our previous subsonic result<sup>13</sup> was based on the unsteady linearized equation, a linear homogeneous equation, in which the mean flow influence is absent. For further discussions on

the subsonic results, we refer to Ref. 13. At any rate, observation of the results in Figs. 7 and 8 indicates that there is definitely a need for further work in the general transonic Mach-number range (i.e.,  $\Gamma \neq 0$  and  $M \neq 1$ ). Moreover, we remark that inspection of the available results for slender wings and bodies<sup>4,5,12,19</sup> show that the stability derivatives exhibit substantial dependence on pitch-axis location, Mach number, and thickness ratio, whereas the derivatives appear to be rather insensitive in the domain of reduced frequency.

Finally, we note that the examples presented in the preceding figures mainly consist of two typical configurations, namely the half-body (e.g., a circular cone) and the full body of revolution (e.g., a parabolic spindle). Our analysis has ignored all viscous effects such as near wake influences attributed to the former configuration and the boundary-layer effects in terms of displacement thickness or the effects of flow separation due to the latter configuration. The inviscid model employed in the present analysis, therefore, remains to be improved for further inclusion of these flow effects. Nonetheless, such considerations are certainly beyond the scope of the present investigation.

### Concluding Remarks

Our analysis has been based on the linearized parabolic equation. Admittedly, this is a crude model which may contain unsatisfactory detail about the local pressure distribution. It is nevertheless a global method, in the sense that the global thickness effect and the low-frequency limits of the stability derivatives can be accounted for expediently. By contrast, Landahl's earlier result produces a logarithmic singularity as  $k$  approaches zero.

Our calculated results appear to be in fairly good agreement with the available experimental data. Also, in their recent study, Stahara and Spreiter<sup>4</sup> indicate favorable agreement in most cases between their results and ours. Particularly, in the very low-frequency limit, both methods yield almost indistinguishable results. However, for ease of application our method is to be preferred. This is because Stahara and Spreiter have used the mixed-type solutions, which require three different types of kernel functions, hence leading to laborious effort in the application of Adams-Sears iteration. Our work only deals with one type of equation, which greatly simplifies the whole procedure. It is believed that, although the present work is based on a global approach, some refinement in the local distribution could be achieved along the line of Hosokawa's nonlinear correction theory. Specifically, we are interested in the influence of the transonic-shock upon the stability derivatives. Some attempts have been made in our earlier work.<sup>5</sup> Our recent study suggests that a more rigorous formulation can be launched, with the shock included, provided that the steady slender-body solution and the associated steady shock structure are known in advance.

### Acknowledgment

This work presents results of research performed for and supported by the Lockheed-Georgia Independent Research Program and in part under NASA Contract NAS8-20082. The first author (DDL) completed the final phase of this work with the partial support of Northrop's Independent Research Program.

### References

- <sup>1</sup>Oswatitsch, K. and Keune, F., "Flow OW Around Bodies of Revolution at Mach Number One," *Proceedings of the Conference on High-Speed Aeronautics*, Jan. 20-22, 1955, Polytechnic Institute of Brooklyn.
- <sup>2</sup>Spreiter, J. R. and Alksne, A. Y., "Slender-Body Theory Based on Approximate Solution of the Transonic Flow Equation," NASA TR R-2, 1959.
- <sup>3</sup>Krupp, J. A. and Murman, E. M., "Computation of Transonic Flows Past Lifting Airfoils and Slender Bodies," *AIAA Journal*, Vol. 10, July 1972, pp. 880-886.
- <sup>4</sup>Stahara, S. S. and Spreiter, J. R., "Research on Unsteady Transonic Flow Theory," *AIAA Journal*, Vol. 14, Oct. 1976, pp. 1402-1408.
- <sup>5</sup>Liu, D. D., Platzer, M. F., and Ruo, S. Y., "On the Calculation of Static and Dynamic Stability Derivatives for Bodies of Revolution at Subsonic and Transonic Speeds," AIAA Paper 70-190, New York, 1970.
- <sup>6</sup>Ruo, S. Y. and Liu, D. D., "Calculation of Stability Derivatives for Slowly Oscillating Bodies of Revolution at Mach 1.0," Lockheed Missiles and Space Company, Huntsville, Ala., LSMC/HREC D1 62375, 1971.
- <sup>7</sup>Ashley, H. and Landahl, M. T., *Aerodynamics of Wings and Bodies*, Addison-Wesley, Inc., Reading, Mass., 1965.
- <sup>8</sup>Platzer, M. F. and Hoffman, G. H., "Quasi-Slender Body Theory for Slowly Oscillating Bodies of Revolution in Supersonic Flow," NASA TN D-3440, June 1966.
- <sup>9</sup>Oswatitsch, K. and Keune, F., "Ein Äquivalenzsatz für nicht-angestellte Flügel kleiner Spannweite in schallnaher Strömung," *Zeitschrift für Flugwissen*, Bd 3, Heft 2, 1955, pp. 29-46.
- <sup>10</sup>Liu, D. D., "Some Approximate Solutions for Oscillating Bodies of Revolution in Nonlinear Transonic Flow," Lockheed Missiles and Space Company, Huntsville, Ala., LMSC/HREC A791499, June 1968.
- <sup>11</sup>Liu, D. D. and Platzer, M. F., "Sonic and Subsonic Flow Past Slowly Oscillating Bodies of Revolution," Lockheed-Georgia Research ER-10221, Oct. 1969.
- <sup>12</sup>Liu, D. D., "On the Not-So-Slender Wing Theory," *AIAA Journal*, Vol. 15, Feb. 1977, pp. 261-263.
- <sup>13</sup>Liu, D. D., Platzer, M. F., and Ruo, S. Y., "Stability Derivatives for Bodies of Revolution at Subsonic Speeds," *AIAA Journal*, Vol. 14, Feb. 1976, pp. 247-250.
- <sup>14</sup>Hsu, P. T. and Ashley, H., "Introductory Study of Airloads on Blunt Bodies Performing Lateral Oscillations," MIT Fluid Dynamics Research Laboratory, Rept. No. 59-9, 1959.
- <sup>15</sup>Landahl, M. T., "Forces and Moments on Oscillating Slender Wing-Body Combination at Sonic Speed," Office of Scientific Research TN 56-109, Feb. 1956.
- <sup>16</sup>Liu, D. D., "Quasi-Slender Body Theory for Unsteady Linearized Transonic Flow past Pointed Bodies of Revolution," Lockheed Missiles and Space Company, Huntsville, Ala., LMSC/HREC A791435, April 1968.
- <sup>17</sup>Hosokawa, I., "A Refinement of the Linearized Transonic Flow Theory," *Journal of the Physics Society of Japan*, Vol. 15, No. 1, 1960, pp. 149-157.
- <sup>18</sup>Landahl, M. T., *Unsteady Transonic Flow*, Pergamon Press, Oxford, 1961.
- <sup>19</sup>Kimble, K. R., Liu, D. D., Ruo, S. Y., and Wu, J. M., "Unsteady Transonic Flow Analysis for Low Aspect Ratio, Pointed Wings," *AIAA Journal*, Vol. 12, April 1974.
- <sup>20</sup>Ruo, S. Y., "Slowly Oscillating Pointed Low Aspect Ratio Wings at Sonic Speed and Thickness Effect," *Zeitschrift für Angewandte Mathematik und Mechanik*, 54, 1974, pp. 119-121.
- <sup>21</sup>Cheng, H. K. and Hafez, M. M., "Transonic Equivalence Rule: A Nonlinear Problem Involving Lift," *Journal of Fluid Mechanics*, Vol. 72, Pt. 4, 1975, pp. 161-187.
- <sup>22</sup>Maeder, P. F. and Thommen, H. U., "Some Results of Linearized Transonic Flow about Slender Airfoils and Bodies of Revolution," *Journal of Aeronautical Sciences*, Vol. 23, No. 2, Feb. 1956, pp. 187-188.
- <sup>23</sup>Wehrend, W., Jr., "An Experimental Evaluation of Aerodynamic Damping Moments of Cones with Different Center of Rotation," NASA TN D-1768, March 1963.
- <sup>24</sup>Yanagizawa, M., "Measurement of Dynamic Stability Derivatives of Cones and Delta-Wings at High Speed," National Aeronautical Laboratory, Tokyo, Japan, TR-172, 1969.
- <sup>25</sup>Ericsson, L. E. and Redding, J. R., "Boundary Layer Transition and Dynamic Sling Interference," *AIAA Journal*, Vol. 8, Oct. 1970, pp. 1886-1888.
- <sup>26</sup>Platzer, M., "Nicht angestellte pulsierende Körper kleiner Streckung in Unter- und Überschallströmung," *ACTA Mechanica*, Vol. 11/1, 1966, pp. 70-89.
- <sup>27</sup>Revell, J. D., "Second-Order Theory for Steady or Unsteady Subsonic Flow Past Slender Lifting Bodies of Finite Thickness," *AIAA Journal*, Vol. 7, June 1969, pp. 1070-1078.
- <sup>28</sup>Zierep, J., "Der Äquivalenzsatz und die Parabolische Methode für Schallnahe Strömungen," *Zeitschrift für Angewandte Mathematik und Mechanik*, Bd 45, Heft 1, 1965, pp. 19-27.
- <sup>29</sup>Adams, M. C. and Sears, W. R., "Slender Body Theory-Review and Extension," *Journal of Aeronautical Sciences*, Vol. 20, No. 2, Feb. 1953, pp. 85-98.